This article was downloaded by:
On: *25 January 2011*
Access details: *Access Details: Free Access*
Publisher *Taylor & Francis*
Informa Ltd Registered in England and Wales Registered Number: 1072954 Registered office: Mortimer House, 37-41 Mortimer Street, London W1T 3JH, UK

Separation Science and Technology
Publication details, including instructions for authors and subscription information:
http://www.informaworld.com/smpp/title~content=t713708471

Adsorptive Removal of Co and Sr Ions from Aqueous Solution by Synthetic Hydroxyapatite Nanoparticles

Bin Ma[a]; Won Sik Shin[a]; Sanghwa Oh[a]; Yeon-Jin Park[a]; Sang-June Choi[a]
[a] Department of Environmental Engineering, Kyungpook National University, Daegu, Korea

Online publication date: 22 February 2010

To cite this Article Ma, Bin , Shin, Won Sik , Oh, Sanghwa , Park, Yeon-Jin and Choi, Sang-June(2010) 'Adsorptive Removal of Co and Sr Ions from Aqueous Solution by Synthetic Hydroxyapatite Nanoparticles', Separation Science and Technology, 45: 4, 453 — 462
To link to this Article: DOI: 10.1080/01496390903484941
URL: http://dx.doi.org/10.1080/01496390903484941

PLEASE SCROLL DOWN FOR ARTICLE

Full terms and conditions of use: http://www.informaworld.com/terms-and-conditions-of-access.pdf

This article may be used for research, teaching and private study purposes. Any substantial or systematic reproduction, re-distribution, re-selling, loan or sub-licensing, systematic supply or distribution in any form to anyone is expressly forbidden.

The publisher does not give any warranty express or implied or make any representation that the contents will be complete or accurate or up to date. The accuracy of any instructions, formulae and drug doses should be independently verified with primary sources. The publisher shall not be liable for any loss, actions, claims, proceedings, demand or costs or damages whatsoever or howsoever caused arising directly or indirectly in connection with or arising out of the use of this material.

Separation Science and Technology, 45: 453–462, 2010
Copyright © Taylor & Francis Group, LLC
ISSN: 0149-6395 print/1520-5754 online
DOI: 10.1080/01496390903484941

Taylor & Francis
Taylor & Francis Group

Adsorptive Removal of Co and Sr Ions from Aqueous Solution by Synthetic Hydroxyapatite Nanoparticles

Bin Ma, Won Sik Shin, Sanghwa Oh, Yeon-Jin Park, and Sang-June Choi
Department of Environmental Engineering, Kyungpook National University, Daegu, Korea

Downloaded At: 08:50 25 January 2011

Hydroxyapatite nanoparticles were synthesized by using the precipitation method with simulated body fluid solution and applied for adsorption of Co^{2+} and Sr^{2+} in aqueous solution. The single- and bi-solute adsorption experiments were performed to evaluate the maximum adsorption capacity of hydroxyapatite nanoparticles for Co^{2+} and Sr^{2+}, the effect of temperature and pH, and the influence of simultaneous presence of other competing metal ion in a binary system. The synthesized hydroxyapatite nanoparticles had high adsorption capacity for Co^{2+} and Sr^{2+} due to a high specific surface area. The maximum adsorption capacity and binding energy of Co^{2+} were higher than those of Sr^{2+} in single-solute adsorption. The extended Langmuir model was fitted well for bi-solute competitive adsorption of Co^{2+} and Sr^{2+} onto the hydroxyapatite nanoparticles. Thermodynamic analysis showed that adsorption occurred spontaneously for both metals and was endothermic for Co^{2+}, but exothermic for Sr^{2+}.

Keywords adsorption; cobalt; hydroxyapatite nanoparticles; strontium; thermodynamic

INTRODUCTION

Radionuclides such as Co^{2+} and Sr^{2+} in low-level radioactive waste (LLRW) are considered as the most dangerous species for human health because of their high transferability, high solubility, long half-lives, and easy accumulation in living organisms (1). Due to these characteristics, the removal of Co^{2+} and Sr^{2+} from waste streams is important before they are discharged into nature. Various treatment techniques such as chemical precipitation, solvent extraction, reverse osmosis, ion-exchange, and adsorption have been developed over the years (2). Adsorption has been commonly used to remove heavy metals from contaminated water (2).

Hydroxyapatite (HAP), one of the apatite minerals with formula $Ca_{10}(PO_4)_6(OH)_2$, is a sparingly soluble, stable, and inexpensive salt which can be easily produced by precipitation from calcium phosphate solution. The crystal structure of HAP allowed many substitutions of divalent cations and retained them for a long time because of its high adsorption capacity for heavy metals, low water solubility, and high stability under reducing and oxidizing conditions (3). Several researchers have reported on the ability of HAP to bind divalent cations and previous studies have shown that synthetic HAP has a high removal capacity for Pb, Zn, Cu, Cd, Co, and Sr from aqueous solutions (4–10). Mechanisms such as ion-exchange, surface complexation, dissolution of HAP, precipitation of metal phosphates, and substitution of Ca in HAP by metals during recrystallization (co-precipitation) have been proposed to explain the adsorption of cations onto HAP from solution (4–6).

Because pure HAP is very limited due to its brittleness, much effort has been made to modify HAP by polymers, especially polymer-assisted synthesis of nano-sized HAP. Nano-sized HAP has been synthesized by a variety of ceramic processing routes including precipitation, sol-gel, hydrothermal processing routes, etc (11,12). However, the precipitation method is more favorable since the method of preparation is very simple, cost-effective, and eco-friendly (11). Although a few studies reported on the adsorption of heavy metals onto normal-sized HAP (5–8,13), currently not much information is available on the adsorption of heavy metals onto HAP nanoparticles (14). Especially, application of HAP nanoparticles on the removal of radioactive heavy metals such as Co and Sr were not fully investigated.

In this study, synthetic HAP nanoparticles were prepared by using the precipitation method in a simulated body fluid (SBF) solution. The physicochemical properties of HAP nanoparticles were examined. The major objectives of this work are to investigate the effect of the initial metal ion concentrations, the initial solution pH, temperature, as well as the presence of competitive metal ion on the removal of Co^{2+} and Sr^{2+} by synthetic HAP nanoparticles from aqueous solution. The adsorption mechanisms were also discussed. The information on the adsorption of Co^{2+} and Sr^{2+} onto HAP nanoparticles under different conditions obtained in this work would be helpful in the remediation of low-level radioactive waste (LLRW).

Received 12 June 2009; accepted 3 November 2009.
Address correspondence to Won Sik Shin, Department of Environmental Engineering, Kyungpook National University, Daegu 702-701, Korea. Tel.: 82-53-950-7584; Fax: 82-53-950-6579. E-mail: wshin@mail.knu.ac.kr

Downloaded At: 08:50 25 January 2011

EXPERIMENTAL

Preparation and Characterization of Adsorbent

The HAP nanoparticles were synthesized by precipitation in growth medium of simulated body fluid (SBF) solution (11). SBF was prepared by dissolving NaCl, $NaHCO_3$, KCl, K_2HPO_4, $MgCl_2$, $CaCl_2$, and Na_2SO_4 in 1 L of distilled and deionized water at 37°C. It should be noted that these reagents should be added one by one after each reagent was completely dissolved in the order listed in Table 1. Thereafter, additional 4.4 g of $CaCl_2$ and 4.14 g of K_2HPO_4 were added to the SBF solution with stirring to produce the white-colored suspension (11). The suspension was stood for 24 hours at 37°C. After carefully decanting the supernatant, the remaining slurry was transferred into a 250 mL Teflon centrifuge bottle (Nalgene) and then centrifuged at 3000 rpm for 20 min. The precipitate was washed with distilled and deionized water three times and with ethanol twice. After all the washing steps, 1 wt% of polyethylene glycol (PEG, MW = 2000) as dispersant and ethanol (precipitate:ethanol = 1:2.5, v/v%) were added to the precipitate in the 250 mL Teflon bottle. After this, the precipitate in the Teflon bottle was treated with ultrosonication (JAC 2010P, Kodo, Korea) for 10 min at 30 kHz. The resulting solid was dried at 50°C for 24 hours and pulverized using a mortar.

The Brunauer-Emmett-Teller (BET) specific surface area (SSA) was measured from N_2 adsorption isotherm by using specific surface area analyzer (Micromeritics, ASAP-2010). The point of zero charge was determined by the batch equilibration technique, using 0.1 M KNO_3 as inert background electrolyte (15).

X-ray diffraction patterns (XRD) were detected by a Philips PW2273 diffractometer and Cu Kα radiation (40 kV, 25 mA) scanning in 2θ range of 10–60° with a step size 0.02° and a time per step of 30 s. The morphology and particle size of HAP nanoparticles were examined by scanning electron microscopy (SEM, Hitachi S-4200). The chemical composition of HAP nanoparticles were revealed by EDS analysis (Horiba, E-MAX EDS detector).

TABLE 1
Chemical composition of SBF solution

SBF solution		
Order	Reagent	Amount
1	NaCl	8.035 g
2	$NaHCO_3$	0.355 g
3	KCl	0.225 g
4	K_2HPO_4	0.176 g
5	$MgCl_2$	0.145 g
6	1.0 M HCl	39 mL
7	$CaCl_2$	0.292 g
8	Na_2SO_4	0.072 g
9	Tris[a]	6.118 g
10	1.0 M HCl	0–5 mL

[a]Tris-hydroxymethyl aminomethane.

Adsorption Experiments

In order to evaluate the maximum adsorption capacity of HAP nanoparticles for Co^{2+} and Sr^{2+} and the influence of simultaneous presence of other metal ion in binary system on the adsorption of individual metal ion onto HAP nanoparticles, the single- and bi-solute adsorption experiment were performed. All chemical solutions were prepared from dissolving $Co(NO_3)_2 \cdot 6H_2O$ (98 + %) and $Sr(NO_3)_2$ (99 + %) (Sigma-Aldrich, Korea) in distilled and deionized water. For a binary system, chemical solutions were prepared by adding both of the metal ions with equimolar concentration into distilled and deionized water. The pH of solution was measured by pH meter (Thermo Orion, model 720A+, USA).

The single-solute adsorption of Co^{2+} and Sr^{2+} by HAP nanoparticles was carried out in batch system at 25°C. 0.1 g of HAP nanoparticles was mixed with approximately 15 mL of stock solution in 15 mL conical centrifuge tube (polyethylene, SPL Labware, Korea). The pH of the adsorbent was adjusted to 5 by using 0.05 M MES buffer solution (heavy metal free) before mixing with stock solution. The pH of the solution was also maintained at 5 ± 0.05 by using 0.05 M MES buffer solution. The exact amount of added solution was measured gravimetrically. The initial metal ion concentrations varied from 1 to 20 mM, in some case, to 30 mM to obtain adsorption isotherm. Thereafter, the samples were placed and shaken in a rotary shaker for 24 hours at 200 rpm to reach equilibrium, After shaking, the samples were centrifuged at 3000 rpm for 20 min and then the supernatants were filtered through 0.2-μm syringe filter (Whatman, cellulose nitrate membrane filter, $\phi = 25$ mm). The adsorbed amounts (q_e) of Co^{2+} and Sr^{2+} were calculated by the difference between the initial and the final metal ion concentration remaining in equilibrium solution after adsorption. ICP-OES (Perkin-Elmer Optima 2100DV) was used to determine metal ion concentration in solution before and after adsorption. All experiments were conducted in duplicate.

The bi-solute adsorption experiments were performed in the same manner as the single-solute adsorption experiments with equimolar concentration of metal ions.

Effect of Temperature

The thermodynamic parameters about the adsorption processes of Co^{2+} and Sr^{2+} onto HAP nanoparticles can be estimated from following equations (16):

$$\Delta G = -RT \ln K_d \quad (1)$$

$$\Delta G = \Delta H - T\Delta S \quad (2)$$

$$\ln K_d = \frac{\Delta S}{R} - \frac{\Delta H}{RT} \quad (3)$$

$$K_d = \frac{q_e}{C_e} \quad (4)$$

where ΔG (J/mol), ΔH (J/mol) and ΔS (J/mol/K), denotes the change of free energy, enthalpy, and entropy, respectively. K_d (mL/g) is the distribution coefficient, R (8.314 J/mol/K) is the gas constant, and T (K) is the absolute temperature. The values of ΔS and ΔH can be calculated from the intercept and the slope of the plot of ln K_d vs. 1/T (17).

Effect of Solution pH

The effect of solution pH was investigated in the pH range of 2–12 at 25°C. 30 mL of 10 mM Co or Sr solution was added into 50 mL conical centrifuge tube (polyethylene, SPL Labware, Korea) containing 0.2 g of HAP nanoparticles. The initial solution pH was adjusted by adding either 0.1 N HNO_3 or 0.1 N NaOH solution. The suspensions were shaken in a rotary shaker at 200 rpm for 24 hours and then filtrated through the 0.2-μm syringe filter and analyzed for final pH and metal ion concentration. The pH of the solution was measured by a pH meter (Thermo Orion, model 720A+, USA).

Adsorption Isotherm Models

Several isotherm models have been developed to analyze the relationship between metal ions adsorbed on the adsorbent and the residual in solution. The Freundlich, Langmuir, and Dubinin-Radushkevich models are most widely used to predict the adsorption isotherm of metal ion onto various adsorbents.

The Freundlich isotherm model is an empirical expression that encompasses the heterogeneity of the surface and an exponential distribution of the sites and their energies. The isotherm has been further extended by considering the influence of adsorption sites and the competition between different ions for adsorption on the available site:

$$q_e = K_F C_e^{N_F} \quad (5)$$

where K_F [(mmol/g)/(mmol/L)^{N_F}] and N_F (–) are Freundlich adsorption parameters related to adsorption affinity and surface heterogeneity, respectively (18).

The Langmuir isotherm model is based on a monolayer adsorption on a surface containing a finite number of binding sites. It assumes uniform energies of adsorption on the surface and no transmigration of adsorbates in the plane of the surface (19). This model is given as:

$$q_e = \frac{q_{mL} b_L C_e}{1 + b_L C_e} \quad (6)$$

where q_e is the amount of adsorbed metal ion by per unit of adsorbent (mmol/g), C_e is the equilibrium metal ion concentration in residual solutions (mmol/L), and q_{mL} (mmol/g) and b_L (L/mmol) are the Langmuir constants related to the maximum adsorption capacity and adsorption energy (19).

The effect of the isotherm shape can be used to predict whether an adsorption system is favorable or unfavorable both in fixed-bed systems as well as in batch processes (20). The dimensionless constant separation factor (or equilibrium parameter) K_R represents the essential features of the Langmuir isotherm and is defined by

$$K_R = \frac{1}{1 + b_L C_0} \quad (7)$$

where K_R is a dimensionless separation factor, C_0 (mmol/L) is initial metal ion concentration, and b_L (L/mmol) is the Langmuir constant. The K_R values indicate the type of isotherm to be unfavorable ($K_R > 1$), linear ($K_R = 1$), favorable ($0 < K_R < 1$), or irreversible ($K_R = 0$) (20).

The Dubinin-Radushkevich (DR) model has been used to describe the adsorption of metal ions onto HAP (21):

$$q_e = q_{mD} \exp(-\beta \varepsilon^2) \quad (8)$$

where q_{mD} (mmol/g) is the maximum adsorption capacity determined by the DR model, β (mol^2/J^2) is the activity coefficient related to mean adsorption energy, and ε is the Polanyi potential, which is equal to

$$\varepsilon = RT \ln(1 + 1/C_e) \quad (9)$$

where R (8.314 J/mol/K) is the gas constant, T (K) is the absolute temperature. The mean adsorption energy, E (kJ/mol), can be calculated using the following relationship:

$$E = \frac{1}{\sqrt{2\beta}} \quad (10)$$

The value of E can be used as a criterion to differentiate the adsorption mechanism when metal ion was adsorbed onto the adsorbent. Ion-exchange is considered as the dominant adsorption mechanism when the value is between $8 \sim 16$ kJ/mol. In the case of $E < 8$ kJ/mol, physical force may affect the adsorption mechanism. For the values of $E > 16$ kJ/mol, adsorption occurs via chemical adsorption (21).

The Langmuir model can be extended to describe the adsorption of metal ion from the binary system onto HAP nanoparticles. In this case, the extended Langmuir model (often called competitive Langmuir model) is expressed as (22):

$$q_{e,i} = \frac{q_{mL,i} b_{L,i} C_{e,i}}{1 + \sum_{j=1}^{N} b_{L,j} C_{e,j}} \quad (11)$$

where $q_{e,i}$ is the equilibrium adsorption of metal ion i onto adsorbent, $C_{e,i}$ is equilibrium concentration of metal ion i

Downloaded At: 08:50 25 January 2011

in the solution, while $q_{mL,i}$ and $b_{L,i}$ are Langmuir constants obtained from the corresponding single metal adsorption isotherms. The extended Langmuir model assumes that competition between different components is only dependent on the concentration ratio. The extended Langmuir model can be applied to predict the adsorption behavior of individual metal ion in a multi-component system, using the single-solute Langmuir parameters.

In order to test the validity of the extended Langmuir model, the sum of square errors (*SSE*) between the experimental data and the theoretically predictive points and the correlation coefficients (R^2) were determined using the following equations (23):

$$SSE = \sum_{i=1}^{N} (q_{i,\text{exp}} - q_{i,pred})^2 \tag{12}$$

$$R^2 = \frac{\sum q_{i,\text{exp}}^2 - SSE}{\sum q_{i,\text{exp}}^2} \tag{13}$$

where $q_{i,exp}$ and $q_{i,pred}$ represent experimental data and theoretically predicted points, respectively.

RESULTS AND DISCUSSION

Characterization of Synthesized HAP Nanoparticles

As listed in Table 2, the synthesized HAP nanoparticles had a high specific surface area (SSA) of 167 m^2/g, larger than that reported by other authors. This indicates that the synthesized HAP nanoparticles are favorable for adsorption of metal ions. The point of zero charge (PZC) of the synthesized HAP nanoparticles was pH 6.7, which is slightly different from that reported by others (see Table 2). This discrepancy may be due to a different synthesis method. The EDS analysis of HAP nanoparticles is shown in Fig. 1. The Ca/P ratio was 1.42, slightly less than 1.67 which is the characteristic for stoichiometric HAP (i.e., $Ca_{10}(PO_4)_6(OH)_2$). The slight calcium deficiency is common for the samples obtained by the wet methods (26).

The crystal structure of HAP nanoparticles was detected by XRD scanning in 2θ range of 10–60° and the obtained pattern was presented in Fig. 2. The pattern of HAP nanoparticles synthesized from SBF solution was similar to the pattern of HAP nanoparticles reported by Cengiz et al. (11).

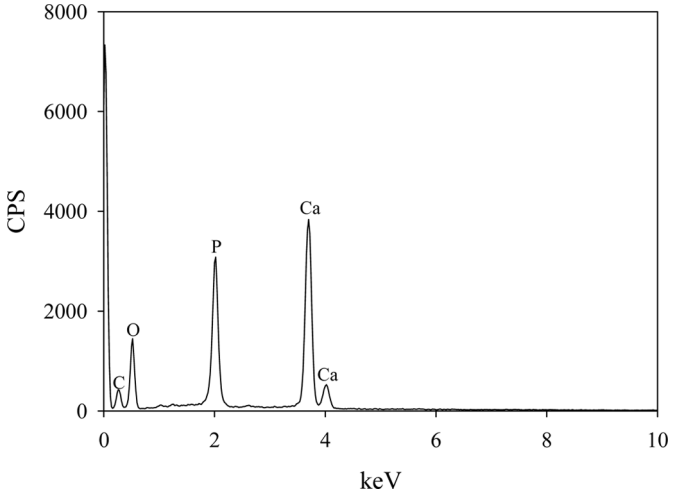

FIG. 1. EDS analysis of HAP nanoparticles.

The SEM photograph of HAP nanoparticles indicates a short-rod like particle shape (Fig. 3). The sizes of most particles are less than 600 nm suggesting that nano-sized HAP particles are successfully synthesized in SBF solution. The nano-sized HAP particles will reduce the diffusion path length of the adsorbate and favor the adsorption of metal ions. The HAP nanoparticles samples have a little aggregated structure indicating that PEG may not perfectly prevent the agglomeration of fine particles.

Single-Solute Adsorption

The single-solute adsorption isotherms of Co^{2+} and Sr^{2+} onto HAP nanoparticles are illustrated in Fig. 4. The metal ion uptake increased with increasing initial metal ion concentrations until it reached equilibrium. This is due to increase in driving force that arises from the concentration gradient (27). The single-solute adsorption experimental data were fitted by Freundlich, Langmuir, and Dubinin-Radushveich (DR) models as shown in Fig. 4 and their parameters are presented in Table 3.

The experimental data was fitted by the Freundlich model which takes into account the heterogeneity of the adsorbent surface. On the basis of the correlation coefficient (R^2: 0.993 for Co^{2+} and 0.989 for Sr^{2+}), the Freundlich model exhibited good performance to predict

TABLE 2
Comparison of physicochemical properties of synthetic HAP

Material	Ca/P ratio	SSA [m^2/g]	pH_{pzc}	Reference
Commercial HAP	1.76	50	7.4	Corami et al. (2)
Synthetic HAP	1.6	67	6.1	Smičiklas et al. (8)
Synthetic HAP	1.6	41	–	Sandrine et al. (24)
Synthetic HAP	1.67	22	6.1	Smičiklas et al. (25)
Synthetic HAP	1.42	167	6.7	This work

Downloaded At: 08:50 25 January 2011

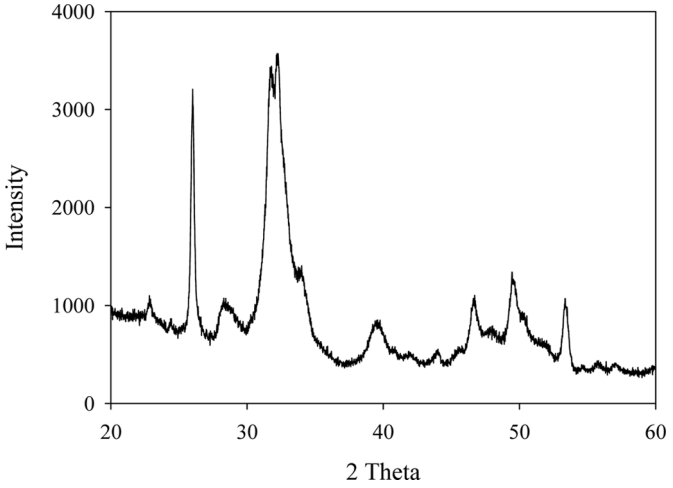

FIG. 2. XRD pattern of HAP nanoparticles.

the single-solute adsorption of Co^{2+} and Sr^{2+} onto HAP nanoparticles. The Freundlich constant (N_F) indicates whether the adsorption process is favorable or not and also deviation from linearity. A relatively slight slope ($N_F << 1$) indicates that the adsorption intensity is favorable over the entire range of concentrations, while a steep slope ($N_F > 1$) means that the adsorption intensity is favorable at high concentration but much less at low concentration (28). In this study, the N_F values for Co^{2+} and Sr^{2+} were 0.413 and 0.519, respectively, representing favorable adsorption over the entire concentration range. The K_F value indicates the adsorption capacity of the adsorbent. The K_F value for Co^{2+} (0.180) was higher than Sr^{2+} (0.084) indicating that Co^{2+} has a relative higher adsorption affinity to HAP nanoparticles than Sr^{2+}.

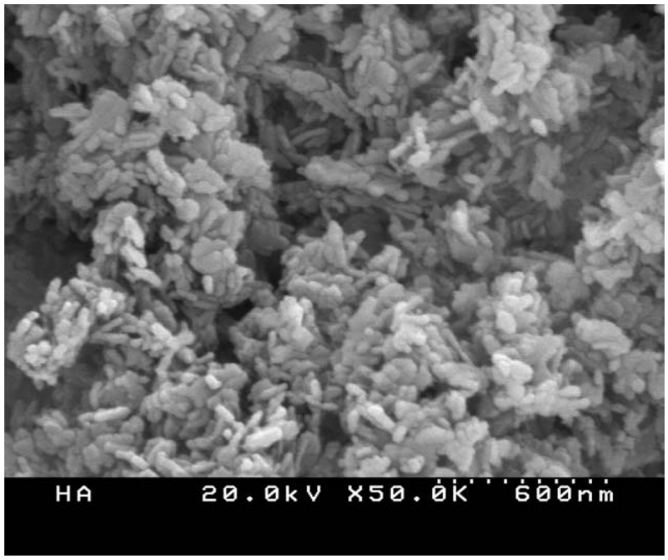

FIG. 3. SEM image of HAP nanoparticles.

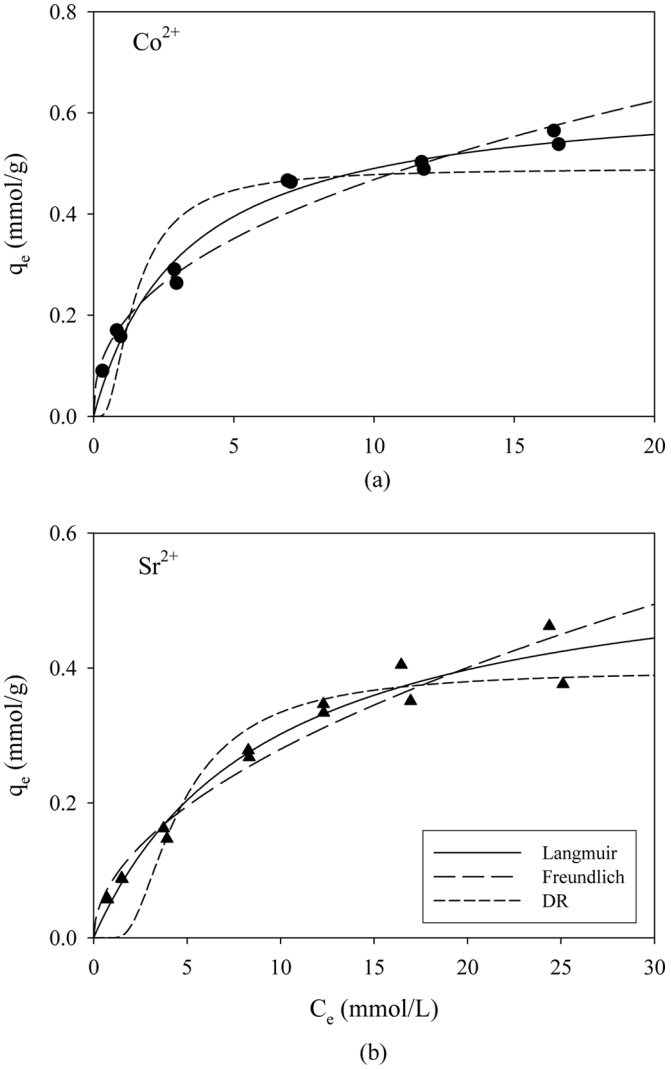

FIG. 4. Single-solute adsorption isotherms for a) Co^{2+} and b) Sr^{2+} onto HAP nanoparticles. Lines represent Freundlich, Langmuir and DR models.

The Langmuir model assumes monolayer coverage of metal ions on the adsorbent surface with a finite number of active sites having identical adsorption energy. The correlation coefficient R^2 (0.996 for Co^{2+} and 0.993 for Sr^{2+}) confirms the excellent agreement between the theoretical model and our experimental results. The maximum adsorption capacity (q_{mL}) values of Langmuir model were 0.645 mmol/g for Co^{2+} and 0.582 mmol/g for Sr^{2+}, respectively. Considering the difference in the physico-chemical properties of adsorbents, these values obtained in this work are higher than those reported by Smiciklas et al. (8) and Lazić and Vuković (10). Smiciklas et al. (8) reported a maximum adsorption capacity of Co^{2+} (0.354 mmol/g) by synthetic HAP. Lazić and Vuković (10) found that HAP could adsorb Sr^{2+} to a limit of 0.150 mmol/g. The higher q_{mL} values (0.645 mmol/g for Co^{2+} and 0.582 mmol/g for Sr^{2+}) in this study could be attributed to higher specific

Downloaded At: 08:50 25 January 2011

Downloaded At: 08:50 25 January 2011

TABLE 3
Single-solute adsorption parameters determined from Langmuir, Freundlich and DR models

	Freundlich				Langmuir				DR			
	K_F [(mmol/g)/(mmol/L)^{N_F}]	N_F [-]	R^2	SSE	q_{mL} [mmol/g]	b_L [L/mmol]	R^2	SSE	q_{mD} [mmol/g]	β [mol^2/J^2]	E [kJ/mol]	R^2	SSE
Co^{2+}	0.180 ± 0.013	0.413 ± 0.032	0.9934	0.011	0.645 ± 0.028	0.315 ± 0.045	0.9958	0.0073	0.490 ± 0.031	4.51E-07	1.050	0.9679	0.0562
Sr^{2+}	0.084 ± 0.010	0.519 ± 0.046	0.9887	0.012	0.582 ± 0.044	0.107 ± 0.019	0.9934	0.0072	0.397 ± 0.024	3.10E-06	0.402	0.9702	0.0325

surface area of HAP nanoparticles synthesized by precipitation in SBF solution than other methods (see Table 2). The b_L values related to the binding energy of active sites were 0.315 L/mmol for Co^{2+} and 0.107 L/mmol for Sr^{2+}, respectively, indicating that HAP nanoparticles preferred to retain Co^{2+} over Sr^{2+}.

Figure 5 shows the plot of the separation factor (K_R) against initial metal ion concentrations. The values of K_R indicates the type of isotherm to be unfavorable ($K_R > 1$), linear ($K_R = 1$), favorable ($0 < K_R < 1$), or irreversible ($K_R = 0$) (29). The calculated K_R values for Co^{2+} and Sr^{2+} are all less than unity indicating that the adsorptions of both metal ions onto HAP nanoparticles are favorable.

The predictive results of DR model are presented in Fig. 4. The maximum adsorption capacity, q_{mD}, determined from this model are 0.490 mmol/g for Co^{2+} and 0.397 mmol/g for Sr^{2+}, respectively, which are lower than q_{mL} values derived from Langmuir model (see Table 3). This difference can be attributed to the different definition of q_m in both models. In the Langmuir model, q_{mL} represents the maximum adsorption capacity of metal ions at monolayer coverage, while q_{mD} represents the maximum adsorption capacity of metal ions at the total specific micropore volume of the adsorbent in DR model (28). Therefore, the q_{mL} value of the Langmuir model is not usually equal to the q_{mD} derived from DR model. The calculated E values for Co^{2+} and Sr^{2+} were 1.05 and 0.402 kJ/mol, respectively, less than 8 kJ/mol. This indicates that the physical adsorption is the primary adsorption process in this study.

Bi-Solute Competitive Adsorption

The simultaneous removal of Co^{2+} and Sr^{2+} by HAP nanoparticles from aqueous solution was studied in a binary system with equimolar concentration and the result

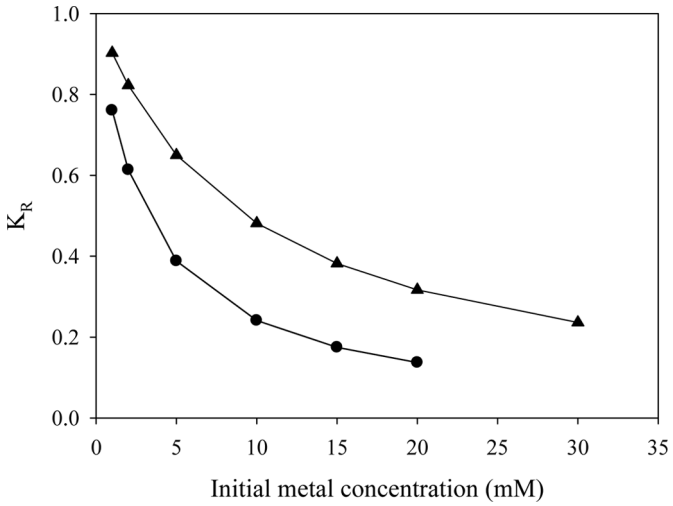

FIG. 5. Separation factor (K_R) for the adsorption of Co^{2+} and Sr^{2+} onto HAP nanoparticles.

Downloaded At: 08:50 25 January 2011

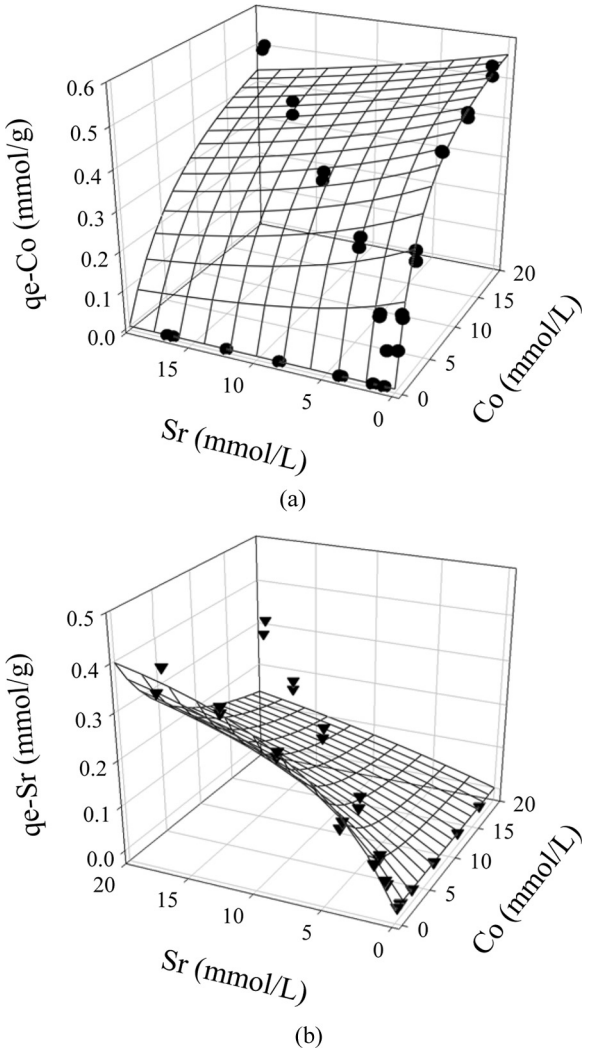

FIG. 6. Binary competitive adsorption of Co^{2+} and Sr^{2+} onto HAP nanoparticles. The mesh surface is predicted by extended Langmuir model.

was presented in Fig. 6 along with mesh surface predicted by extended Langmuir model. The correlation coefficient (R^2) and SSE for Co^{2+}/Sr^{2+} were 0.9793/0.9020 and 0.067/0.164, respectively.

The most appropriate way to represent the experimental results of bi-solute competitive adsorption is to draw 3D plots where the uptake of each metal ion is plotted as a function of the final equilibrium concentrations of two metal ions. It should be noted that the single adsorption isotherm of each metal ion can be seen in the respective main vertical planes, where the concentration of the other metal ion is zero (23). As shown in Fig. 6, for both metal ions, the uptake of each metal ion was suppressed by the presence of other metal ion indicating that Co^{2+} and Sr^{2+} compete for binding sites in binary system. The sum of the maximum adsorption capacity of Co^{2+} and Sr^{2+} in a binary system is lower than the sum of their corresponding maximum adsorption capacity in a single-solute solution (1.03 mmol/g < 1.22 mmol/g). For that reason, the adsorption sites on the surface of HAP nanoparticles for Co^{2+} and Sr^{2+} may be partially overlapped. It may also display the existence of specific adsorption sites on the surface of HAP nanoparticles towards individual metal ions (27). In Fig. 6, the extended Langmuir model would tend to overestimate the influence of Co^{2+} on the adsorption of Sr^{2+}, while the prediction for the adsorption of Co^{2+} fits the experimental data well. The R^2 values (=0.9793 for Co^{2+} and 0.9020 for Sr^{2+}) for the binary system indicate that the extended Langmuir model fitted bi-solute adsorption experimental data adequately.

The effect of the simultaneous presence of competing metal ion on the adsorption of single metal ion can be represented by the ratio of the adsorption capacity of one metal ion in the binary system, q^*_{mL}, to the adsorption capacity of the corresponding metal ion in single-solute solution, q_{mL}. Indeed, when the ratio is greater than 1 the adsorption is promoted by the presence of other metal ions; when the ratio is equal to 1 there is no observable competitive effects; when the ratio is less than 1 the adsorption is hindered by the presence of other metal ions. The q^*_{mL}/q_{mL} values for Co^{2+} (=0.910) and Sr^{2+} (=0.768) are less than unity as shown in Table 4 suggesting that the simultaneous presence of both metal ions in binary system decreased the adsorption of each metal ion onto HAP nanoparticles through competition for surface active sites (30). This is further

TABLE 4
Comparison of q_{mL} and b values of single-solute and bi-solute competitive adsorption

Binary system (1)/(2)[a]	$q_{mL,1}/q_{mL,2}$[b]	$q^*_{mL,1}/q^*_{mL,2}$	$q^*_{mL,1}/q_{mL,1}$	$q^*_{mL,2}/q_{mL,2}$
Co^{2+}/Sr^{2+}	1.109	1.315	0.910	0.768
Binary system (1)/(2)	$b_{L,1}/b_{L,2}$	$b^*_{L,1}/b^*_{L,2}$	$b^*_{L,1}/b_{L,1}$	$b^*_{L,2}/b_{L,2}$
Co^{2+}/Sr^{2+}	2.922	2.360	1.142	1.414

[a]The metal ions in binary system labeled in the order of (1) and (2).
[b]q_{mL} and b_L: Langmuir constants for single-solute adsorption.
[c]q^*_{mL} and b^*_L: Langmuir constants for bi-solute competitive adsorption.

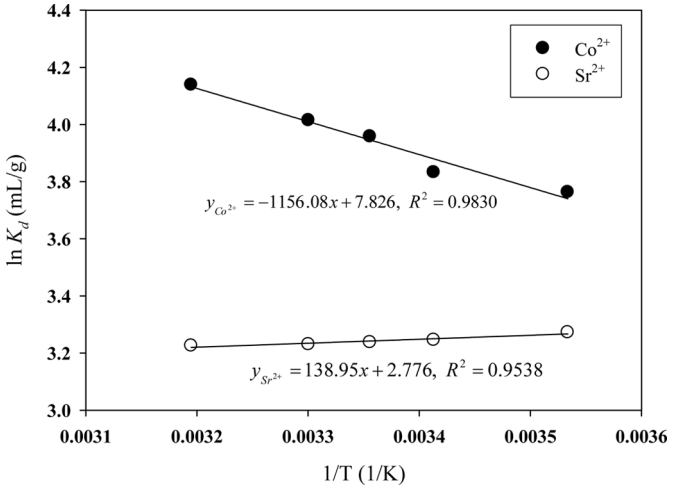

FIG. 7. Thermodynamic plots of ln K_d against 1/T for the adsorption of Co^{2+} and Sr^{2+} onto HAP nanoparticles.

supported by the value of $q_{mL,Co}/q_{mL,Sr}$ (=1.109) which is lower than that of $q^*_{mL,Co}/q^*_{mL,Sr}$ (=1.315). In addition, it is generally true that $q^*_{mL,Sr}/q_{mL,Sr} < q^*_{mL,Co}/q_{mL,Co}$ suggesting that the adsorption of Sr^{2+} onto HAP nanoparticles was more affected by the simultaneous presence of competing metal ion than Co^{2+} (2,20,21).

According to $b_{L,1}/b_{L,2}$ and $b^*_{L,1}$ / $b^*_{L,2}$ ratios presented in Table 4, the binding energy coefficient showed greater adsorption affinity for Co^{2+} than Sr^{2+} as $b_{L,Co} > b_{L,Sr}$ for single-solute adsorption and $b^*_{L,Co} > b^*_{L,Sr}$ for bi-solute adsorption. In addition, the b^*_L/b_L ratios for Co^{2+} and Sr^{2+} were 1.142 and 1.414, respectively, meaning that competition for the adsorption sites could promote the retention of Co^{2+} and Sr^{2+} on more specific adsorption sites. As a result, the maximum adsorption capacities of Co^{2+} and Sr^{2+} in a bi-solute system were lower than those in a single-solute system, whereas Co^{2+} and Sr^{2+} were held more strongly in the bi-solute system than in the single-system.

Effect of Temperature

The effect of temperature on the adsorption of Co^{2+} and Sr^{2+} onto HAP nanoparticles was investigated from 283 K to 313 K and plotted in Fig. 7. The thermodynamic parameters are listed in Table 5.

TABLE 5
Thermodynamic parameters for the adsorption of Co^{2+} and Sr^{2+} onto HAP nanoparticles

			ΔG [kJ/mol]				
Metal	ΔH[kJ/mol]	ΔS [kJ/mol/K, $\times 10^{-3}$]	283 K	293 K	298 K	303 K	313 K
Co^{2+}	9.61	65.07	−8.80	−9.45	−9.78	−10.10	−10.75
Sr^{2+}	−1.15	23.07	−7.69	−7.91	−8.03	−8.14	−8.38

The enthalpy change ΔH is a measure of the energy barrier that must be overcome by the metal ion during adsorption onto adsorbent (31). The positive value of ΔH for Co^{2+} (=9.61 kJ/mol) indicates that the adsorption of Co^{2+} onto HAP nanoparticles is an endothermic process. In contrast, the adsorption of Sr^{2+} onto HAP nanoparticles decreased with increasing temperature suggesting an exothermic adsorption process ($\Delta H = -1.15$). This means that Sr^{2+} will liberate from the adsorbent to the solution with the rise in temperature.

The entropy change ΔS for Co^{2+} and Sr^{2+} are found to be 65.07 kJ/mol and 23.07 kJ/mol, respectively, which reveal some structure change between the adsorbent and the adsorbate during adsorption reaction. In addition, the positive values of ΔS indicate the increasing randomness at the solid-liquid interface during the adsorption of both cations onto HAP nanoparticles (32).

The negative values of ΔG show that the adsorptions of Co^{2+} and Sr^{2+} onto HAP nanoparticles are spontaneous in nature and the degree of spontaneity increase with increasing temperature. This may be attributed to the increase in the number of active surface sites available for metal ions and the decrease in the thickness of the boundary layer surrounding the adsorbent which will accelerate the mass transfer process (28).

Effect of Initial Solution pH

The adsorption and precipitation of Co^{2+} as a function of initial solution pH was examined over a pH range of 2–12 and the results are presented in Fig. 8. The adsorption of Co^{2+} onto HAP nanoparticles increased with increasing initial solution pH up to 9 and then reached a plateau at pH range of 9–12 where precipitation, not adsorption, contributed to 98% disappearance of Co^{2+} from solution. The adsorption of Co^{2+} was hindered by the presence of competitive H^+ as pH decreased, resulting in relative low adsorption capacity (0.23 mmol/g). The removal of Co^{2+}

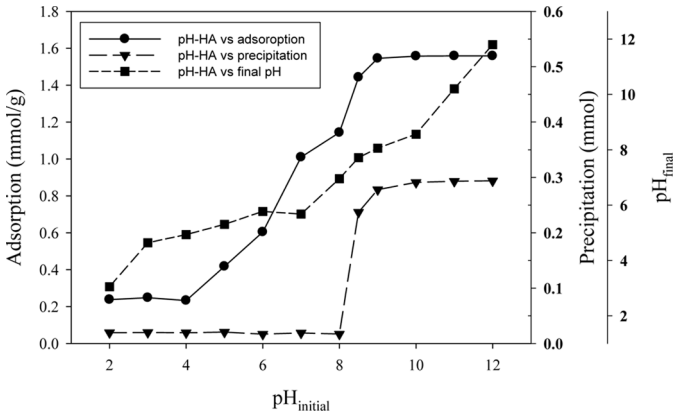

FIG. 8. The influence of initial solution pH on the adsorption and precipitation of Co^{2+} and final pH.

Downloaded At: 08:50 25 January 2011

Downloaded At: 08:50 25 January 2011

at low pH may be attributed to the partial dissolution of HAP nanoparticles with subsequent precipitation of a Co-containing hydroxyapatite with formula $Co_xCa_{10-x}(PO_4)_6(OH)_2$ (2). It is noticeable that a sharp increase of Co^{2+} adsorption was observed in the pH range of 4–8. This may be due to a rapid formation of $CoOH^+$ in this pH range and the adsorption process was quickly completed by interaction with negative charge sites by surface complexation. Smiciklas et al. (8) reported that in the initial solution pH range of 4–8 cobalt is removed from the solution through ion-exchange with HAP. The disagreement on the adsorption mechanisms may be caused by different physico-chemical properties of HAP prepared by different methods and experimental conditions.

The amount of Sr^{2+} adsorbed onto HAP nanoparticles under different initial solution pH and the final pH values as well as the precipitation of Sr^{2+} are presented in Fig. 9. In the pH range of 2–12, the contribution of precipitation to the total adsorption was negligible, except at pH 12. Wu et al. showed that when $pH < pH_{pzc}$, ≡POH are the significant surface species, whereas at pH close to and higher than pH_{pzc}, the dominant surface sites are $\equiv PO^-$ and ≡CaOH (33). In the low pH range of 2–6 (below pH_{pzc}), the pH increase results from consumption of H^+ from solution by protonation of surface sites $\equiv PO^-$ and ≡CaOH. The removal of Sr^{2+} in this pH range is probably due to ion-exchange ($Sr_xCa_{10-x}(PO_4)_6(OH)_2$) or surface complexation with ≡POH. It is obvious that the adsorption of Sr^{2+} onto HAP nanoparticles decreases the final pH around the pH_{pzc} value in the pH range of 6–10 through the following reactions (34):

$$HA - OH + Sr^{2+} \rightarrow HA - OSr^+ + H^+ \quad (14)$$

$$2HA - OH + Sr^{2+} \rightarrow (HA - O)_2Sr + 2H^+ \quad (15)$$

which suggests the surface complexation as a dominant adsorption mechanism.

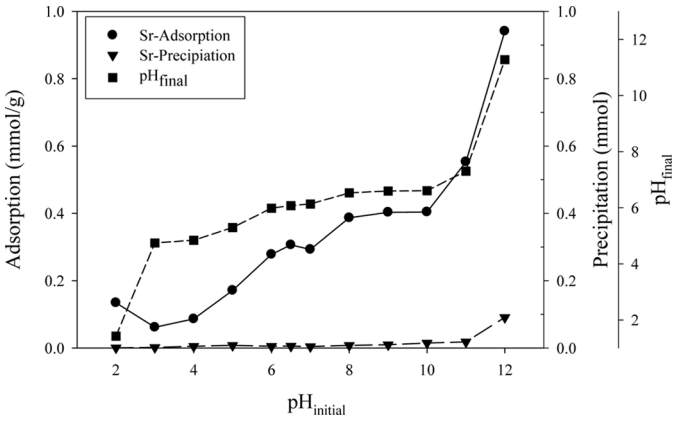

FIG. 9. The influence of initial solution pH on the adsorption and precipitation of Sr^{2+} and final pH.

At pH above 10, where the surface of HAP nanoparticles becomes negatively charged, the sharp increase of adsorption is accelerated by the negative charge on adsorbent surface and partially by precipitation of $Sr(OH)_2$. The ion-exchange process became unfavorable at $pH > 10$ because of the increased stability of HAP nanoparticles in an alkaline environment (35).

CONCLUSIONS

The HAP nanoparticles synthesized by the simple precipitation method using SBF solution were highly effective in the adsorptive removal of Co^{2+} and Sr^{2+} due to high specific surface area. The Langmuir, Freundlich, and Dubinin-Radushkevich model parameters obtained from curve-fitting indicated that the single-solute adsorptions of Co^{2+} and Sr^{2+} onto HAP nanoparticles were favorable. The maximum adsorption capacity and binding energy of Co^{2+} were higher than those of Sr^{2+}. In a binary system, the adsorption of Sr^{2+} was more affected than Co^{2+} by the simultaneous presence of competing metal ion in solution. The extended Langmuir model was found to fit competitive adsorption data adequately.

The adsorption of Co^{2+} onto HAP nanoparticles was endothermic indicating that increase in temperature will favor this reaction. In contrast, the adsorption of Sr^{2+} was exothermic indicating that decrease in temperature promotes the removal of Sr^{2+}. The positive values of ΔS for Co^{2+} and Sr^{2+} show some structural change between the adsorbent and the adsorbate during the adsorption processes. The negative values of ΔG denote that adsorptions of Co^{2+} and Sr^{2+} onto HAP nanoparticles are spontaneous in nature and the degree of spontaneity increase with increasing temperature.

The adsorptions of Co^{2+} and Sr^{2+} onto HAP nanoparticles were strongly dependent on initial solution pH. Ion-exchange and surface complex formation are considered as major adsorption mechanisms for the removal of Co^{2+} and Sr^{2+} by HAP nanoparticles.

ACKNOWLEDGEMENT

This study was financially supported by Korea Science and Engineering Foundation (KOSEF) of the Korean Ministry of Education, Science, and Technology (Grant Number: M20706000036-07M0600-03610) and by the second stage of the Brain Korea 21 Project in 2010.

REFERENCES

1. Singh, S.; Eapen, S.; Thorat, V.; Kaushik, C.P.; Raj, K.; D'Souza, S.F. (2008) Phytoremediation of ^{137}cesium and ^{90}strontium from solutions and low-level nuclear waste by *Vetiveria zizanoides*. *Ecotoxicol. Environ. Saf.*, 69: 306–311.
2. Corami, A.; Mignardi, S.; Ferrini, V. (2008) Cadmium removal from single- and multi-metal (Cd+Pb+Zn+Cu) solutions by sorption on hydroxyapatite. *J. Colloid Interf. Sci.*, 317: 402–408.
3. Krestou, A.; Xenidis, A.; Panias, D. (2004) Mechanism of aqueous uranium(VI) uptake by hydroxyapatite. *Miner. Eng.*, 17: 373–381.

4. Ma, Q.Y.; Traina, S.J.; Logan, T.J.; Ryan, J.A. (1994) Effects of aqueous Al, Cd, Cu, Fe(II), Ni, and Zn on Pb immobilization by hydroxyapatite. *Environ. Sci. Technol.*, 28: 1219–1228.
5. Xu, Y.; Schwartz, F.W.; Traina, S.J. (1994) Sorption of Zn^{2+} and Cd^{2+} on hydroxyapatite surfaces. *Environ. Sci. Technol.*, 28: 1472–1480.
6. Leyva, A.G.; Marrero, J.; Smichowski, P.; Cicerone, D. (2001) Sorption of antimony onto hydroxyapatite. *Environ. Sci. Technol.*, 35: 3669–3675.
7. Gómez del Río, J.A.; Morando, P.J.; Cicerone, D.S. (2004) Natural materials for treatment of industrial effluents: comparative study of the retention of Cd, Zn and Co by calcite and hydroxyapatite. Part I: batch experiments. *J. Environ. Manage.*, 71: 169–177.
8. Smičiklas, I.; Dimović, S.; Plećaš, I.; Mitrić, M. (2006) Removal of Co^{2+} from aqueous solutions by hydroxyapatite. *Water Res.*, 40: 2267–2274.
9. Yasukawa, A.; Yokoyama, T.; Kandori, K.; Ishikawa, T. (2007) Reaction of calcium hydroxyapatite with Cd^{2+} and Pb^{2+} ions. *Colloids Surf. A: Physicochem. Eng. Aspects*, 299: 203–208.
10. Lazić, S.; Vuković, Ž. (1991) Ion exchange of strontium on synthetic hydroxyapatite. *J. Radioanal. Nucl. Chem.*, 149: 161–168.
11. Cengiz, B.; Gokce, Y.; Yildiz, N.; Aktas, Z.; Calimli, A. (2008) Synthesis and characterization of hydroxyapatite nanoparticles. *Colloids Surf. A: Physicochem. Eng. Aspects*, 322: 29–33.
12. Tseng, Y.H.; Kuo, C.S.; Li, Y.Y.; Huang, C.P. (2009) Polymer-assisted synthesis of hydroxyapatite nanoparticle. *Mater. Sci. Eng., C*, 29: 819–822.
13. Šljivić, M.; Smićiklas, I.; Plećaš, L.; Mitrić, M. (2009) The influence of equilibration conditions and hydroxyapatite physic-chemical properties onto retention of Cu^{2+} ions. *Chem. Eng. J.*, 148: 80–88.
14. Wang, Y.J.; Chen, J.H.; Cui, Y.X.; Wang, S.Q.; Zhou, D.M. (2009) Effects of low-molecular-weight organic acids on Cu(II) adsorption onto hydroxyapatite nanoparticles. *J. Hazard. Mater.*, 162: 1135–1140.
15. Čerović, Lj.S.; Milonjić, S.K.; Todorović, M.B.; Trtanj, M.I.; Pogozhev, Y.S.; Blagoveschenskii, Y.; Levashov, E.A. (2007) Point of zero charge of different carbides. *Colloids Surf. A: Physicochem. Eng. Aspects*, 297: 1–6.
16. Abou-Mesalam, M.M. (2003) Sorption kinetics of copper, zinc, cadmium and nickel ions on synthesized silico-antimonate ion exchanger. *Colloids Surf. A: Physicochem. Eng. Aspects*, 225: 85–94.
17. Ghiaci, M.; Kalbasi, R.J.; Khani, H.; Abbaspur, A.; Shariatmadari, H. (2004) Fee-energy of adsorption of a cationic surfactant onto Na-bentonite (Iran): inspection of adsorption layer by X-ray spectroscopy. *J. Chem. Thermodyn.*, 36: 707–713.
18. Willms, C.; Li, Z.; Allen, L.; Evans, C.V. (2004) Desorption of cesium from kaolinite and illite using alkylammonium salts. *Appl. Clay Sci.*, 25: 125–133.
19. Adebowale, K.O.; Unuabonah, I.E.; Olu-Owolabi, B.I. (2006) The effect of some operating variables on the adsorption of lead and cadmium ions on kaolinite clay. *J. Hazard. Mater.*, 134: 130–139.
20. Unuabonah, E.I.; Olu-Owolabi, B.I.; Adebowale, K.O.; Ofomaja, A.E. (2007) Adsorption of lead and cadmium ions from aqueous solutions by tripolyphosphate-impregnated kaolinite clay. *Colloids Surf. A: Physicochem. Eng. Aspects*, 292: 202–211.
21. Erdem, E.; Karapinar, N.; Donat, R. (2004) The removal of heavy metal cations by natural zeolites. *J. Colloid Interf. Sci.*, 280: 309–314.
22. Al-Asheh, S.; Banat, F.; Al-Omari, R.; Duvnjak, Z. (2000) Predictions of binary sorption isotherms for the sorption of heavy metals by pine bark using single isotherm data. *Chemosphere*, 41: 659–665.
23. Papageorgiou, S.K.; Katsaros, F.K.; Kouvelos, E.P.; Kanellopoulos, N.K. (2009) Prediction of binary adsorption isotherms of Cu^{2+}, Cd^{2+} and Pb^{2+} on calcium alginate beads from single adsorption data. *J. Hazard. Mater.*, 162: 1347–1354.
24. Sandrine, B.; Ange, N.; Didier, B.A.; Eric, C.; Patrick, S. (2007) Removal of aqueous lead ions by hydroxyapatites: Equilibria and kinetic processes. *J. Hazard. Mater.*, 139: 443–446.
25. Smičiklas, I.D.; Milonjić, S.K.; Pfendt, P.; Raičević, S. (2000) The point of zero charge and sorption of cadmium (II) and strontium (II) ions on synthetic hydroxyapatite. *Sep. Purif. Technol.*, 18: 185–194.
26. Narasaraju, T.S.B.; Phebe, D.E. (1996) Some physico-chemical aspects of hydroxyapatite. *J. Mater. Sci.*, 31: 1–21.
27. Srivastava, V.C.; Mall, I.D.; Mishra, I.M. (2008) Removal of cadmium(II) and zinc(II) metal ions from binary aqueous solution by rice husk ash. *Colloids Surf. A: Physicochem. Eng. Aspects*, 312: 172–184.
28. Eren, E.; Afsin, B.; Onal, Y. (2009) Removal of lead ions by acid activated and manganese oxide-coated bentonite. *J. Hazard. Mater.*, 161: 677–685.
29. Zheng, H.; Wang, Y.; Zheng, Y.; Zhang, H.; Liang, S.; Long, M. (2008) Equilibrium, kinetic and thermodynamic studies on the sorption of 4-hydroxyphenol on Cr-bentonite. *Chem. Eng. J.*, 143: 117–123.
30. Mohan, D.; Chander, S. (2000) Single component and multi-component adsorption of metal ions by activated carbons. *Colloids Surf. A: Physicochem. Eng. Aspects*, 177: 183–196.
31. Unuabonah, E.I.; Adebowale, K.O.; Olu-Owolabi, B.I.; Yang, L.Z.; Kong, L.X. (2008) Adsorption of Pb(II) and Cd(II) from aqueous solutions onto sodium tetraborate-modified kaolinite clay: Equilibrium and thermodynamic studies. *Hydrometallurgy*, 93: 1–9.
32. Unuabonah, E.I.; Adebowale, K.O.; Olu-Owolabi, B.I. (2007) Kinetic and thermodynamic studies of the adsorption of lead(II) ions onto phosphate-modified kaolinite clay. *J. Hazard. Mater.*, 144: 386–195.
33. Wu, L.; Forsling, W.; Schindler, P.W. (1991) Surface complexation of calcium minerals in aqueous solution: 1. Surface protonation at fluorapatite-water interfaces. *J. Colloid Interf. Sci.*, 147: 178–185.
34. Corami, A.; Mignardi, S.; Ferrini, V. (2007) Copper and zinc decontamination from single- and binary-metal solutions using hydroxyapatite. *J. Hazard. Mater.*, 146: 164–170.
35. Smiciklas, I.; Dimovic, S.; Sljivic M.; Plecas, I. (2008) The batch study of Sr^{2+} sorption by bone char. *J. Environ. Sci. Health. Part A Toxic/Hazard. Subst. Environ. Eng.*, 43: 210–217.

Downloaded At: 08:50 25 January 2011